Comparison between conventional and lost foam compound casting of Al/Mg light metals

S. M. Emami, M. Divandari*, E. Hajjari and H. Arabi

The microstructure obtained in conventional and lost foam compound casting of Al/Mg alloy was examined and compared. X-ray diffraction, optical and SEM examinations showed that casting magnesium melt around the aluminium insert, in both methods, is caused formation of an interface consisting three different layers. Layer I, beside aluminium consists of Al_3Mg_2 intermetallic compound, layer II consists of $Al_{12}Mg_{17}$ phase and layer III, in the vicinity of magnesium, is formed of $Al_{12}Mg_{17}+(Mg)$ eutectic. The result of Vickers microhardness tests, at the interface zones, showed that the hardness of the middle layer is increased substantially (200–250 HV) in comparison to the hardness of the base metals, namely aluminium and magnesium. Using the LFC method reduced the thickness of interface as a result of both, lowering the temperature and the speed of melt. The mean thicknesses of the interface in the conventional and LFC processes were 600 and 200 μm respectively.

Keywords: Compound casting, Lost foam casting, Interface, Aluminium, Magnesium

Introduction

Compound casting is a process of joining two metals or alloys via direct casting in which one component is in the solid state, as a core, and the other as pouring metal. In such a manner, a diffusion reaction zone between the two metals, and thus a continuous metallic transition, from one metal to the other can be formed.[1–3] This method is used for joining semifinished parts with complex structures, simply by casting a metal onto or around a solid shape.[4] Despite these benefits, the joining process of metals like aluminium and magnesium, by the compound casting process, is associated with many problems and constraints such as formation of oxide layers on the surface and precipitation of undesirable intermetallic compounds.[5–8] Production of a composite bimetal part with the appropriate properties is required to overcome these problems.

Lost foam casting (LFC) has been used as a production process for more than 50 years. In this process the embedded polystyrene pattern in the sand mould is decomposed by molten metal. So, the molten metal replaces the polystyrene pattern and duplicates all features of the pattern.[9] Currently, many casting facilities are dedicated strictly to the lost foam process because of its interesting and numerous advantages such as no mould parting line, no cores, more accurate dimensions, no environmental pollutants, ability to produce complex pieces and also cost reduction.[10–12] An interesting advantage of this process is the possibility of mounting the desired solid part inside the polystyrene pattern (coring) and performing the casting process afterwards. Divandari *et al.*[13,14] used LFC method to study different dissimilar metallic couples, such as aluminium/copper and cast iron/copper, and studied the microstructure and properties of the obtained products. Also Cho *et al.*[15] used the lost foam compound casting (LFCC) in order to join aluminium and steel. Thus, this method can be used for the production of parts with desirable mechanical and physical properties and may lead to spread the application of this process.

Magnesium and aluminium are the first and second engineering light metals respectively and are attractive in vehicle structure applications for improving energy efficiency which reduces the emission of greenhouse gases. In many cases, one of these materials alone does not satisfy the requirements of lightweight constructions, and dissimilar joining between these two metals must be faced.[16] However, many researchers have used the compound casting in order to join different dissimilar and similar metallic couples such as steel/cast iron,[17,18] steel/Cu,[19] steel/Al,[15,20] Cu/Al,[13] Al/Al,[3,20,21] and Mg/Mg,[22] but joining dissimilar light metals such as aluminium and magnesium, by compound casting process, is still a relatively unexplored area. A good contact with satisfactory metallurgical and mechanical properties between Mg/Al, Al/Al and Mg/Mg couples, leads to significant increase in application of these light metals in automotive and aerospace industries which results in lower fuel consumption.[21,23]

In this work, the conventional compound casting (CCC) and LFCC processes for the dissimilar joining of Al/Mg light metals were studied. Bonding conditions including microstructure characteristics and microhardness were examined in order to evaluate

School of Metallurgy and Materials Engineering, Iran University of Science and Technology (IUST), Narmak, Tehran, Iran

*Corresponding author, email divandari@iust.ac.ir

Received 20 February 2012; accepted 27 August 2012
DOI 10.1179/1743133612Y.0000000037

and compare CCC and LFCC processes for joining these two metals.

Experimental procedure

Commercially pure aluminium and magnesium were used to prepare Al/Mg couples by the compound casting process. Mean chemical compositions of the materials used are listed in Table 1.

In order to fabricate the Al/Mg couples by the compound casting process cylindrical inserts, with 20 mm diameter and 100 mm height, were machined from aluminium ingots. Their surface were ground with the silicon carbide papers up to 1200 grit, then rinsed with acetone and placed within a cylindrical cavity of a CO_2 sand mould with 40 mm diameter and 80 mm height. Schematic of the mould used in the casting process and the prepared Al/Mg couple are illustrated in Fig. 1. Gating system in the CCC and in the LFCC processes were made with wood and polystyrene (EPS with a density of 0·02 g cm^{-3}) patterns respectively.

Magnesium ingots were melted in a steel crucible placed in an electrical resistance furnace under the Foseco MAGREX 36 covering flux to protect magnesium melt from oxidation. The molten magnesium was cast around the aluminium inserts at 700°C under normal atmospheric conditions.

After the casting, specimens were cut from the bottom, middle and top parts of the samples, perpendicular to the cylindrical insert, using an electrical discharge machine (Fig. 2). Then the middle parts polished with 1 μm diamond paste. Owing to nature of dissimilar metals bond, specimens were etched by 1 vol.-%HNO_3 in alcohol solution on the magnesium side and 1 vol.-%HF in distilled water solution on the aluminium side. Specimens were examined using a JEOL JSM-7000F scanning electron microscope (SEM) equipped with the energy dispersive X-ray (EDS) detector. The phase constitutions on the fracture surfaces of the specimens were also identified by using a Rigaku RINT-RAPID X-ray diffractometer. In addition, a Buehler hardness tester with a testing load of 50 g and a holding time of 20 s was used to determine the Vickers microhardness profile across the joint interface.

Results and discussion

Figure 3 shows SEM images from samples prepared by casting magnesium melt around the aluminium insert, using CCC process and LFCC process.

As can be seen in Fig. 3, a relatively uniform interface has been formed due to contact between magnesium melt and the aluminium insert that consist of three different reaction layers. These are a layer at the aluminium side (layer I), a middle layer (layer II) and the layer at the magnesium side (layer III). Also Fig. 3 shows that the thickness of reaction layer, in the case of LFC, is about one-third of the conventional casting

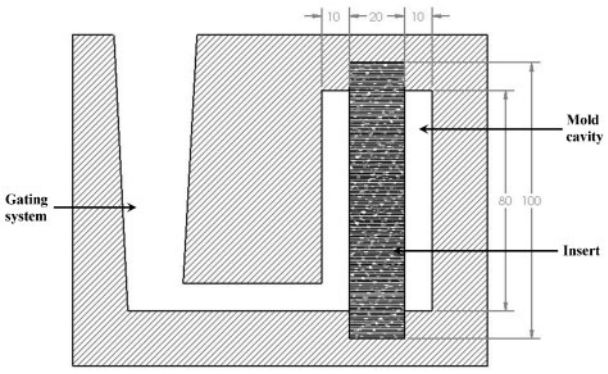

1 Schematic of mould used for casting process

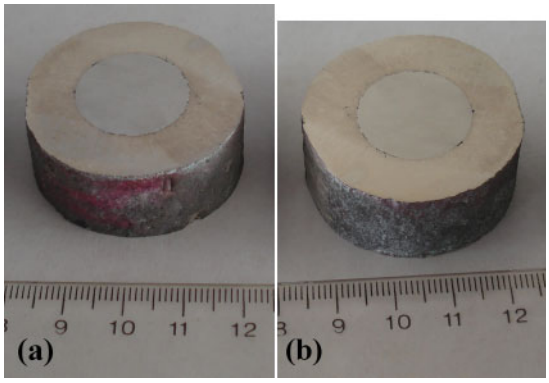

a sample prepared by conventional casting; *b* sample prepared by LFC

2 Cross-section of Al/Mg joint in compound casting process

method. Therefore, the reaction layer thickness reduces from 600 μm in CCC to 200 μm in LFCC.

X-ray diffraction pattern of the constitutive phases, on the fracture surface of the Al/Mg joint, (Fig. 4) confirms the formation of two Mg phases, Al_3Mg_2 and $Al_{12}Mg_{17}$ intermetallic compounds, within the interface microstructure.

In order to study the interfacial microstructure of the Al/Mg couples in the compound casting process, the reaction layers were examined using EDS, line scan and X-ray map analysis. Figures 5 and 6 show a typical EDS map of the elements Al, Mg and O in the CCC and LFCC cast samples respectively.

Figure 7 shows line scans of the elements Al and Mg in the samples produced by CCC and LFCC. As shown in these figures, the magnesium content gradually decreases across interface from its base toward aluminium insert and it is exactly vice versa for aluminium.

It is noteworthy that across the interface, the curve corresponding to magnesium (upper line) is almost above the curve corresponding to aluminium (lower line) except in a small region of the interface close to aluminium (layer I). This indicates that compounds

Table 1 Mean chemical compositions of commercial metals, used in this study/wt-%

	Al	Mg	Zn	Sn	Mn	Cu	Fe	Si
Commercially pure aluminium	99·548	0·027	0	0·076	0·009	0·002	0·0171	0·131
Commercially pure magnesium	0	99·847	0·093	0	0·017	0·012	0·002	0·029

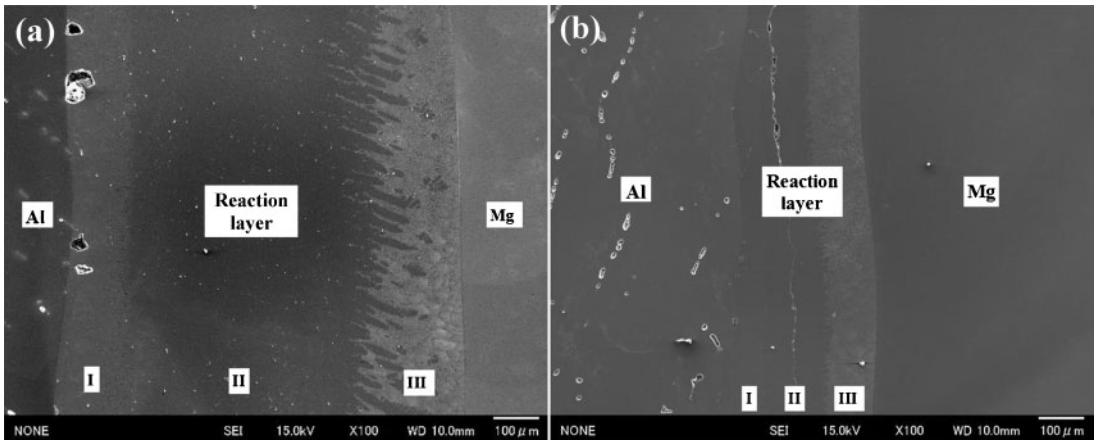

a conventional casting; *b* LFC

3 Images (SEM) of interfacial microstructures from Al/Mg joint in compound casting process

with higher Mg content, comprise a large portion of the microstructure.

Quantitative analysis results of aluminium and magnesium elements by EDS in 10 different areas (A1–A10 in Fig. 8) of the interface between the aluminium insert and magnesium melt by CCC process and LFCC process are listed in Tables 2 and 3 respectively.

According to these results, the layer on the aluminium side (layer I) is mainly composed of the Al_3Mg_2 intermetallic compound, while the $(Al_{12}Mg_{17}+\delta)$ eutectic structure due to $L \xrightarrow{437\,^{\circ}C} Al_{12}Mg_{17}+\delta$ eutectic transformation is the main constituent of the layer on the magnesium side (layer III). In layer II unlike layers I and III, which almost have constant chemical compositions, the ratio of aluminium and magnesium for different areas of the layer is not constant and varies from 0·611 to 1·021. Considering the relatively wide range of the composition for the $Al_{12}Mg_{17}$ intermetallic compound in the Al-Mg binary phase diagram (45–60 at-%Mg) shown in Fig. 9, it seems that the middle layer (layer II) is mainly composed of the $Al_{12}Mg_{17}$ intermetallic compound. This is in agreement with the reports from other researchers.[7,16,24,25] Thus, the microstructure of reaction layers in the interface can be distinguished as Figs. 10 and 11.

According to images shown above, a microstructural defect in the interface of the lost foam cast specimen can be seen (Fig. 11*a*). This is a thin oxide film which often forms on the surface of Mg and Al alloys. Figure 6*d* confirms the presence of oxygen in the contact area of these two metals.

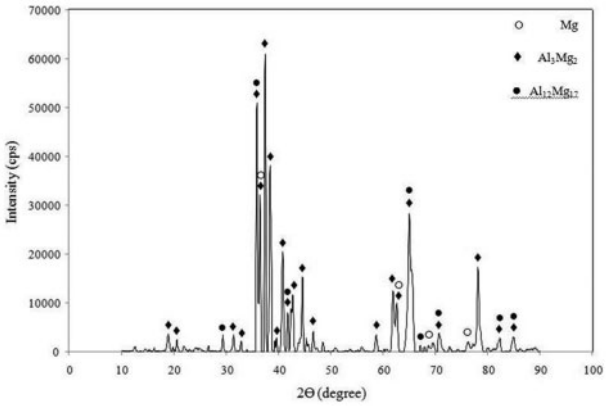

4 X-ray diffraction patterns of constitutive phases on fracture surface of Al/Mg joint in compound casting process

Another possible mechanism, on the formation of this defect, is the entrapment of gaseous and liquid products as a result of foam dissociation in the liquid front.[27] As the melt temperature decreases and dendrites form, the pyrolytic products (based on their volume) may either entrapped in the melt or reach the surface and form a layer on the surface or inside the part. The higher the concentration of dissociation products, formed in a certain volume, the more the extent of this defect would be.[28]

From the thermodynamic viewpoint, owing to the negative standard Gibbs free energy, magnesium melt can react with the thin aluminium oxide layer on the surface of aluminium insert and reduce it according to the reaction below[29]

$$\mathrm{Mg_{(l)}}+\frac{1}{3}\mathrm{Al_2O_{3\ (s)}}\rightarrow \mathrm{MgO_{(s)}}+2/3\mathrm{Al_{(l)}} \qquad (1)$$
$$\Delta G^0=-39\ \mathrm{kJ\ mol^{-1}\ Mg\ at\ 1000\ K}$$

This can cause removing the oxide layer from the surface of the aluminium insert and thus make direct contact between the magnesium melt and the fresh surface of aluminium insert, and lead to the formation of an interfacial layer between them.

Formation of different layers, with various compositions, between the aluminium insert and the magnesium melt implies that diffusion is the dominant mechanism for mass transportation, in the compound casting process, as is the case with solid state diffusion bonding. During this process the heat of melt leads to melting the surface layer of cylindrical insert, and then concentration gradient causes the aluminium and magnesium melts to diffuse into each other. After that, according to the Al–Mg binary phase diagram (Fig. 9), intermetallic compounds such as Al_3Mg_2 and $Al_{12}Mg_{17}$ can form, within the interface, after finishing the solidification.

In the LFC process, by the time melt is cast over the polystyrene pattern, foam undergoes sudden dissociation through complex reactions. The products of dissociation affect melt flow, mould filling, heat transfer, solidification and microstructure of cast part, defects, etc.[30]

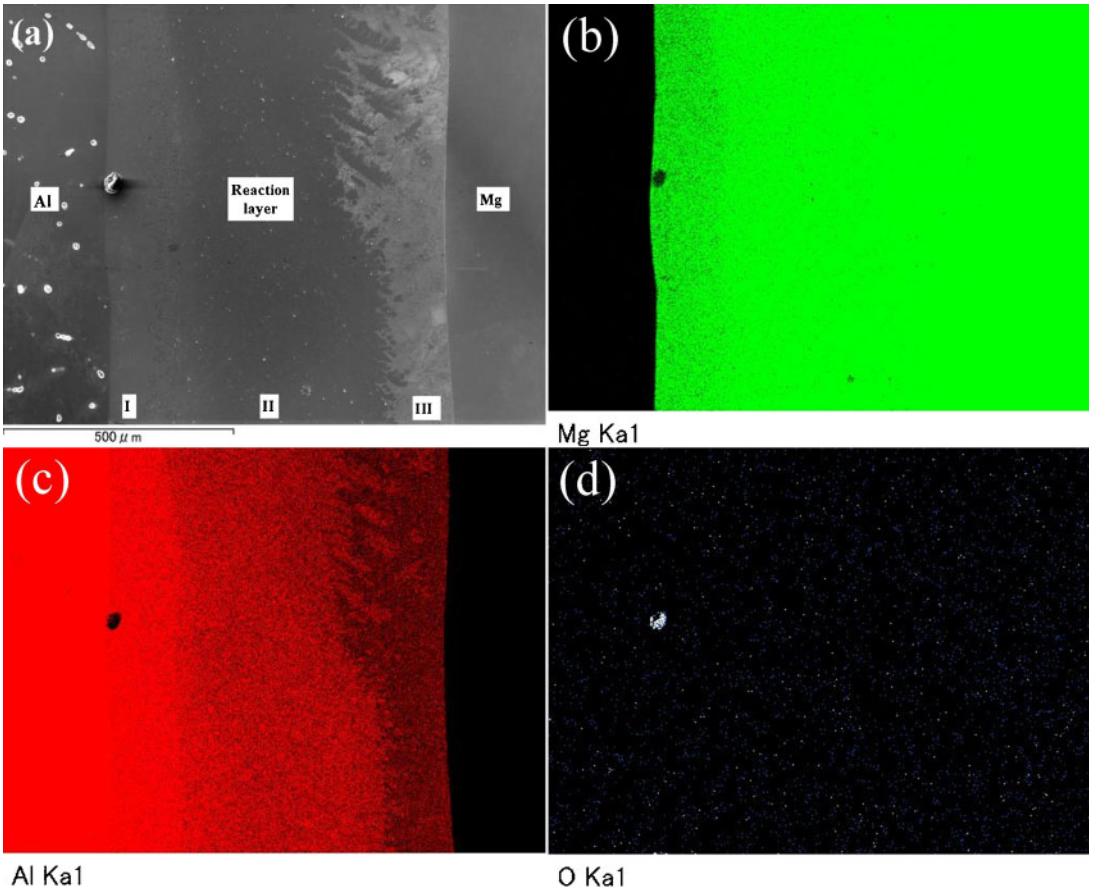

a SEM micrograph; *b* Mg distribution map; *c* Al distribution map; *d* O distribution map

5 Energy dispersive X-ray maps of Al, Mg and O on cross-section of Al/Mg joint in CCC process

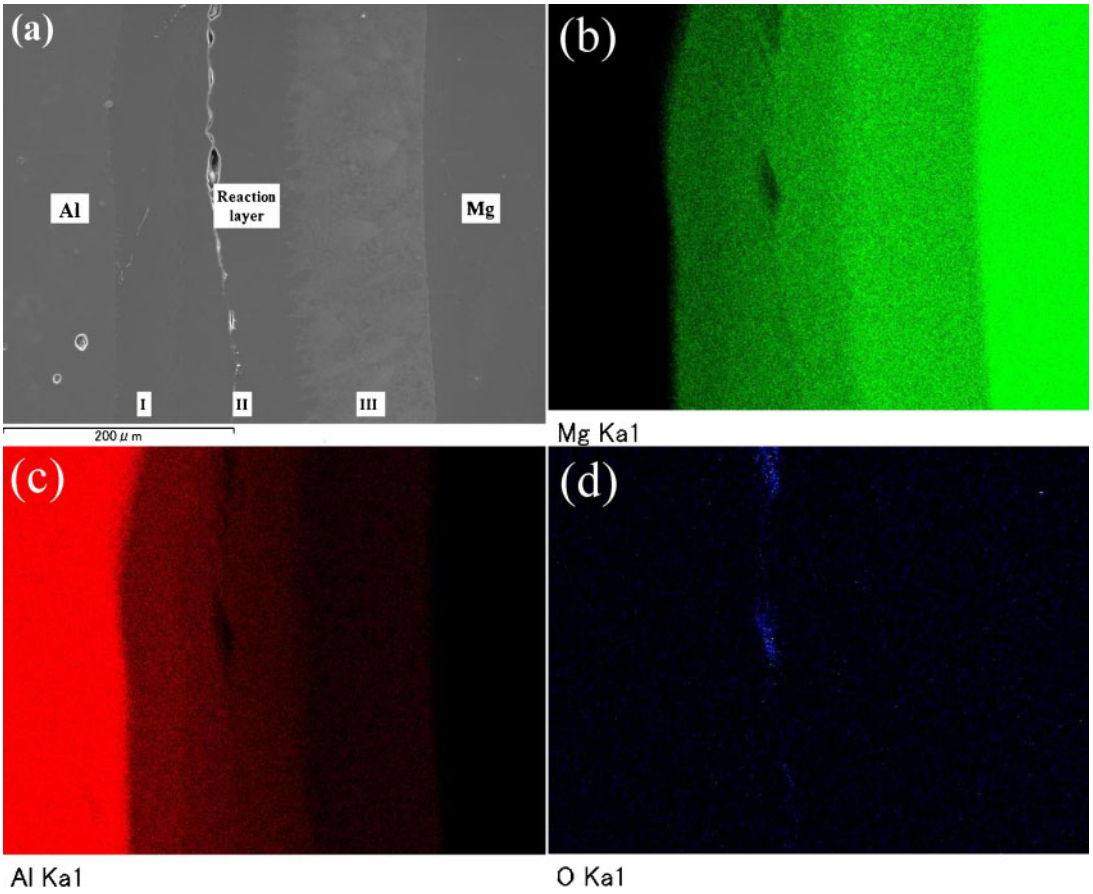

a SEM micrograph; *b* Mg distribution map; *c* Al distribution map; *d* O distribution map

6 Energy dispersive X-ray maps of Al, Mg and O on cross-section of Al/Mg joint in the LFCC process

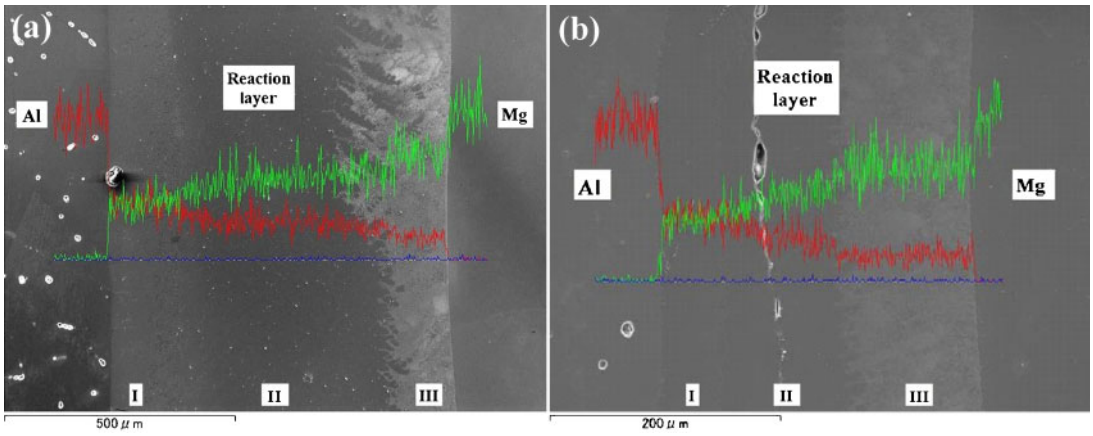

a conventional casting; *b* LFC

7 Energy dispersive X-ray line scan of cross-section of Al/Mg joint in compound casting process

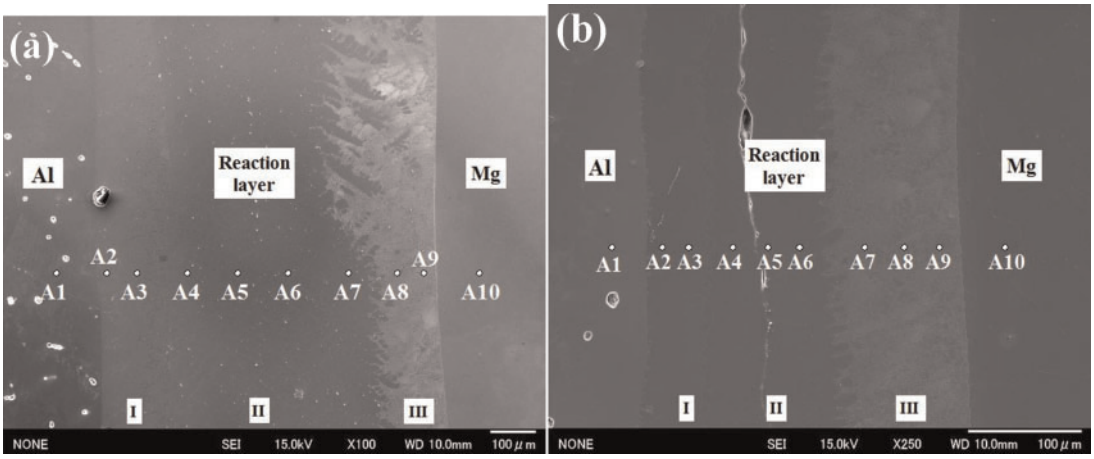

8 Location of points analysed in interface of specimen prepared by *a* conventional casting and *b* LFC

As it is evident in Fig. 3 and already pointed out, the interface formed through lost foam process is thinner than that of formed in conventional cast process. It seems that the LFC process reduces the reaction layer thickness in the solid/liquid interface by two mechanisms i.e. reducing melt temperature and velocity and as a result of the postponement of the contact time between melt and solid insert.

Reducing melt temperature

To replace the polystyrene pattern by melt, in the LFC process, foam pattern has to undergo dissociation and disappear. The energy needed, for the foam dissociation, is supplied by the melt thermal energy which firstly melts down the foam and then raises its temperature to dissociation temperature.[31]

Various researchers have calculated and determined the energy needed for dissociation of various foams by using different methods.[32–34] Among them, one can mentioned Tseng and Askeland[35] whom obtained the energy required for polystyrene foam dissociation with density of 0·025 g cm^{-3} as 30·86 J cm^{-3}.

On the other hand, melt enthalpy can be calculated from the equation below[36]

Table 2 Energy dispersive X-ray quantitative analysis results of Al and Mg elements at Al/Mg interface corresponding to points indicated in Fig. 8*a*

		Element compositions/at-%			
Area no.	Layer code	Al	Mg	Element compositions ratio (Al/Mg)	Inference component
A1	…	100	0	…	Al
A2	I	59·98	40·02	1·499	Al_3Mg_2
A3		58·78	41·22	1·426	Al_3Mg_2
A4	II	50·53	49·47	1·021	$Al_{12}Mg_{17}$
A5		43·85	56·15	0·781	$Al_{12}Mg_{17}$
A6		42·48	57·52	0·738	$Al_{12}Mg_{17}$
A7		37·94	62·06	0·611	$Al_{12}Mg_{17}$
A8	III	28·19	71·81	0·392	$Al_{12}Mg_{17}$+(Mg)*
A9		27·16	72·84	0·373	$Al_{12}Mg_{17}$+(Mg)*
A10	…	0	100	…	Mg

*(Mg) is magnesium solid solution.

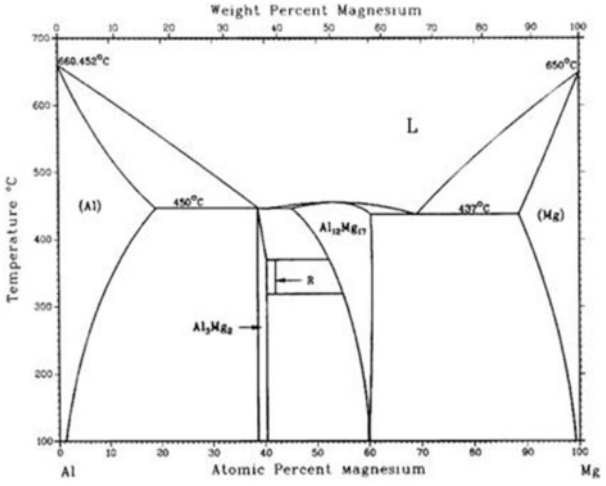

9 Al–Mg binary phase diagram[26]

and equals 1360 J kg^{-1} K^{-1} and the density of magnesium is $1{\cdot}738 \times 10^{-3}$ kg cm^{-3},[3,36] therefore, the heat content due to magnesium melt superheat of 50°C, for 1 cm^3 magnesium melt, can be calculated as below

$$\Delta H = 1{\cdot}783 \times 10^{-3} \times 1360 \times 50 = 118{\cdot}18 \text{ J} \quad (3)$$

The answer equals the energy needed for increasing the temperature of 1 cm^3 magnesium melt from 650 to 700°C. In another word, it is heat content of 1 cm^3 magnesium melt above its melting temperature.

By comparing this value (i.e. 118·18 J) to the energy needed for foam dissociation (i.e. 30·86 J) it can be easily concluded that in the Mg LFC process, almost 26% of magnesium melt heat content, above its melting temperature, will be used to dissociate polystyrene foam in the cavity. This phenomenon reduces Mg melt temperature by 13°C and as a result reduces the contact time and the reaction layer thickness in the interface between Mg melt and Al insert.

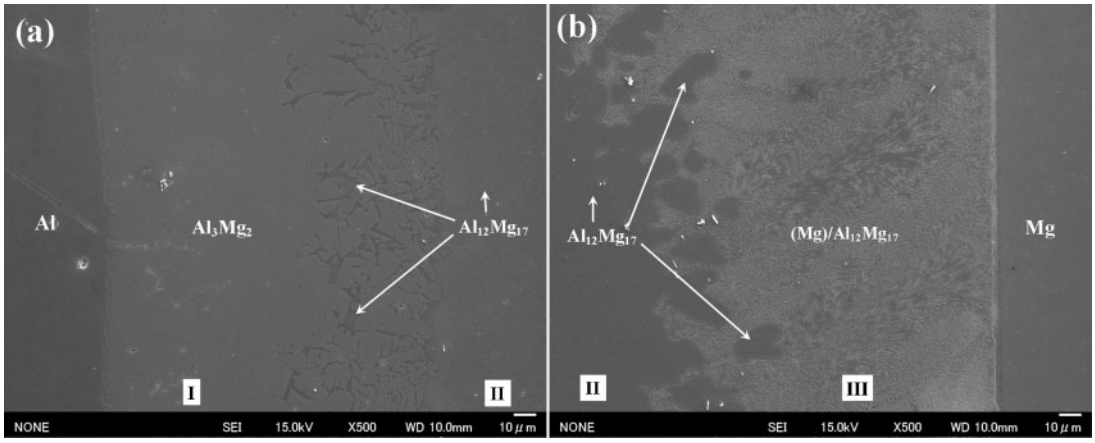

a vicinity of aluminium metal; *b* vicinity of magnesium metal

10 Microstructure of interface formed in Al/Mg specimen prepared by conventional casting process

$$\Delta H = \int_{T_1}^{T_2} m\,c\,\mathrm{d}T \quad (2)$$

where m is mass, c the specific heat capacity and T the melt temperature.

Since the specific heat capacity c of magnesium in the range 650–700°C is almost independent of temperature

Delay in contact time between melt and solid insert

As soon as the melt enters the mould, the polystyrene pattern dissociates and produces various gases. These gases fill the mould, apply a pressure on the melt and reduce the melt velocity. In addition, they hinder the rapid contact between melt and solid insert to some extent and reduce the contact time between them.[32,37–40]

Table 3 Energy dispersive X-ray quantitative analysis results of Al and Mg elements at Al/Mg interface corresponding to points indicated in Fig. 8*b*

		Element compositions/at-%			
Area no.	Layer code	Al	Mg	Element compositions ratio (Al/Mg)	Inference component
A1	…	100	0	…	Al
A2	I	60·17	39·83	1·511	Al_3Mg_2
A3		59·78	40·22	1·486	Al_3Mg_2
A4	II	48·00	52·00	0·923	$Al_{12}Mg_{17}$
A5		45·90	54·10	0·848	$Al_{12}Mg_{17}$
A6		42·41	57·59	0·736	$Al_{12}Mg_{17}$
A7	III	30·99	69·01	0·449	$Al_{12}Mg_{17}$+(Mg)*
A8		28·98	71·02	0·408	$Al_{12}Mg_{17}$+(Mg)*
A9		27·18	72·82	0·373	$Al_{12}Mg_{17}$+(Mg)*
A10	…	0	100	…	Mg

*(Mg) is magnesium solid solution.

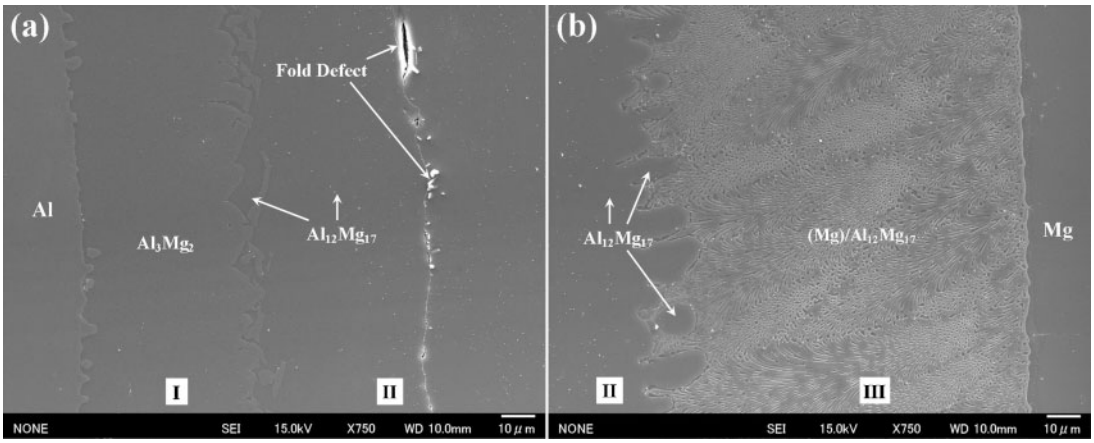

a vicinity of aluminium metal; *b* vicinity of magnesium metal

11 Microstructure of interface formed in Al/Mg specimen prepared by LFC process

On the other hand, in order to substitute the polystyrene foam surrounding Al insert with the Mg melt, all the gases created during the thermal decomposition of the foam, should be evacuated from the mould. Therefore, depending on the flow of these gases exiting the mould, there is a time delay before the melt gets into contact with the aluminium insert. This can reduce the time, which the melt is in contact with the insert, and finally result in a reduction of the interface thickness.

A schematic representation of how the gas products of foam dissociation hinder melt progress and as a result reduce melt velocity is presented in Fig. 12.

In addition to reducing interface thickness, the presence of foam in the mould reduces the unwanted and low melting point intermetallic compounds in the interface. As already pointed out, due to the contact between melt and foam and its dissociation melt temperature, the reduced velocity of the melt weakens the melt reaction with the solid insert. Therefore, there will be no sufficient time for these phases to form, especially in the last steps of solidification.

The results of microhardness distributions, taken from the interface zone of the two samples, are shown in Fig. 13. As can clearly be seen in Fig. 13, microhardness distributions are consistent with the microstructures of the interface. For both samples, the hardness of the interface is significantly higher than those of the aluminium and magnesium base metals. The microhardness ranges from 152 to 252 HV, depending on the position of indenter relative to interface location, while the base metals of aluminium and magnesium have average hardness values of 30 and 40 HV respectively.

Higher hardness of the interface, relative to the aluminium and magnesium base metals, confirms that harder Al–Mg intermetallic compounds have been formed within the Al/Mg interface.[5,41] The higher hardness values, in the specimen prepared by CCC process, can be the result of an increase in the reaction volume of Al/Mg that causes the formation of more intermetallic compounds, with higher hardness, during the solidification stage. Moreover, according to Fig. 13, the microhardness of the interface at the magnesium side (layer III) is lower than that of the aluminium side (layer I); and the intermediate area (layer II, i.e. $Al_{12}Mg_{17}+\delta$) eutectic structure has lower hardness than the $Al_{12}Mg_{17}$ and Al_3Mg_2 intermetallic compounds, due to the presence of magnesium solid solution. This is in agreement with the reports from Liu *et al.*,[5] Hajjari *et al.*[16] and Dietrich *et al.*[42]

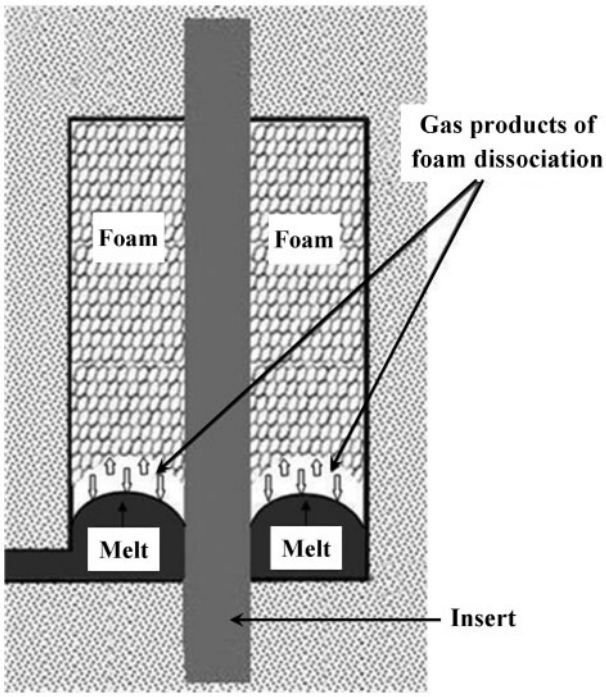

12 Schematic illustration of contact between melt and foam, gas products and reduction of melt temperature and velocity

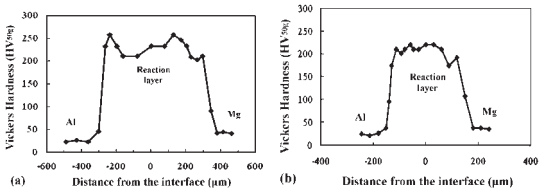

13 Microhardness distributions from interface zone of *a* conventional casting process and *b* LFC process

Conclusions

1. Joining of aluminium and magnesium by the compound casting process is feasible by both conventional casting and LFC methods.

2. Formation of the interface in the compound casting process is diffusion controlled and the interface consists of three different layers. The layers adjacent to the aluminium and magnesium base metals are composed of the Al_3Mg_2 intermetallic compound and the $(Al_{12}Mg_{17}+\delta)$ eutectic structure respectively, and the middle layer is composed of the $Al_{12}Mg_{17}$ intermetallic compound.

3. Dissimilar joining of Al/Mg light metals by LFCC process reduces the interface thickness and the volume of undesirable intermetallic compounds compared to that of CCC process.

4. For both samples, the hardness of the interface is significantly higher than those of aluminium and magnesium base metals; this can be an indication of the fact that the high hardness Al–Mg intermetallic compounds were formed within the Al/Mg interface.

References

1. B. K. Amoid, T. Heijkoop, P. G. Lloyd, G. Rubenis and I. R. Sare: *Wear*, 1997, **203–204**, 663–670.
2. K. J. M. Papis, J. F. Loeffler and P. J. Uggowitzer: *Sci. China Ser. E: Tech. Sci.*, 2009, **52**, 46–51.
3. K. J. M. Papis, B. Hallstedt, J. F. Loeffler and P. J. Uggowitzer: *Acta Mater.*, 2008, **56**, 3036–3043.
4. N. Horikawa, T. Ito, T. Noguchi and T. Nakamura: *Inter. J. Cast. Met. Res.*, 2003, **16**, 365–369.
5. P. Liu, Y. Li, H. Geng and J. Wang: *Mater. Lett.*, 2007, **61**, 1288–1291.
6. L. M. Liu, H. Y. Wang and Z. D. Zhang: *Scr. Mater.*, 2007, **56**, 473–476.
7. L. Peng, L. Yajiang, G. Haoran and W. Juan: *Vacuum*, 2006, **80**, 395–399.
8. R. Zettler, A. Augusto, M. D. Silva, S. Rodrigues, A. Blanco and J. F. D. Santos: *Adv. Eng. Mater.*, 2006, **8**, 415–421.
9. in 'ASM metals handbook', 'Casting', 15; 1992, Materials Park, OH, ASM International.
10. H. B. Dieter: *AFS Trans.*, 1990, **98**, 943–946.
11. F. Sonnenberg: *AFS Trans*, 2003, **111**, 006–008.
12. R. S. Benson, D. Penumada, I. Sen and R. Michaels: *AFS Trans.*, 2004, **112**, 54–65.
13. M. Divandari, and A. R. VahidGolpayegani: *Mater. Des.*, 2009, **30**, 3279–3285.
14. M. Hejazi, M. Divandari and E. Taghaddos: *Mater. Des.*, 2009, **30**, 1085–1092.
15. K. H. Choe, K. S. Park, B. H. Kang, G. S. Cho, K. Y. Kim, K. W. Lee, M. H. Kim, A. Ikenaga, and S. Koroyasu: *J. Mater. Sci. Technol.*, 2008, **24**, 60–64.
16. E. Hajjari, M. Divandari, S. H. Razavi, S. M. Emami, T. Homma and S. Kamado: *J. Mater. Sci.*, 2011, **46**, 6491–6499.
17. T. Noguchi, S. Kamota, T. Sato and M. Sakai: *AFS Trans.*, 1993, **89**, 231–239.
18. A. Avci, N. Ilkaya, M. Simsir, and A. Akdemir: *J. Mater. Process. Technol.*, 2009, **209**, 1410–1416.
19. J. S. Ho, C. B. Lin and C. H. Liu: (2004) *J. Mater. Sci.*, 2004, **39**, 2473–2480.
20. J. Pan, M. Yoshida, G. Sasaki, H. Fukunaga, H. Fujimura and M. Matsuura: *Scr. Mater.*, 2000, **43**, 155–159.
21. M. Scanlan, D. J. Browne and A. Bates: *Mater. Sci. Eng. A*, 2005, **A413**, 66–71.
22. K. J. M. Papis, J. F. Loffler and P. J. Uggowitzer: *Mater. Sci. Eng. A*, 2010, **A527**, 2274–2279.
23. T. Noguchi, N. Horikawa, H. Nagate, T. Nakamura and K. Sato: *Int. J. Cast Met. Res.*, 2005, **18**, 214–220.
24. D. Singh, C. Suryanarayana, L. Mertus and R. H. Chen: *Intermetallics*, 2003, **11**, 373–376.
25. J. R. Cahoon: *Metall. Mater. Trans. B*, 2007, **38B**, 109–112.
26. in 'ASM hand book', Vol. 3, 'Alloy phase diagrams', 9th edn; 1995, Materials Park, OH, ASM International.
27. M. A. Tschopp, Jr, C. W. Ramsay and D. R. Askeland: *AFS Trans.*, 2000, **108**, 614–699.
28. O. Gordugan, H. Huang, H. U. Akay, W. W. Fincher and V. E. Wilson: *AFS Trans.*, 1996, **104**, 451–459.
29. B. Hallstedz, Z. K. Liu and J. Agren: *J. Mater. Sci. Eng. A*, 1990, **A129**, 135–145.
30. C. H. E. Tseng and D. R. Askeland: *AFS Trans.*, 1992, **100**, 509–519.
31. M. R. Barone and D. A. Caulk: *Int. J. Heat Mass. Trans.*, 2005, **48**, 4132–4149.
32. S. Shivkumar and B. Gallois: *AFS Trans.*, 1987, **95**, 791–800.
33. T. V. Molibog and H. Littelton: *AFS Trans.*, 2002, **110**, 1483–1496.
34. S. Mehta and S. Shivkumar: *JMEPEG*, 1994, **3**, 329–333.
35. C. H. E. Tseng and D. R. Askeland: *AFS Trans.*, 1992, **100**, 519–527.
36. D. R. Gaskell: 'Introduction to the thermodynamics of materials', 4th edn; 2003, New York, Taylor & Francis.
37. L. M. Liu, H. Y. Wang and Z. D. Zhang: *Scr. Mater.*, 2007, **56**, 473–476.
38. S. Shivkumar: *Mater. Sci. Technol.*, 1994, **10**, 986–992.
39. S. Saghi, M. Divandari and Y. H. K. Kharrazi: *Iran. J. Mater. Sci. Eng.*, 2004, **1**, 2.
40. Y. H. K. Kharrazi, M. Divandari and S. Saghi: *Iran. J. Mater. Sci. Eng.*, 2005, **2**, 1.
41. Y. S. Sato, S. Hwan, C. Park, M. Michiuchi and H. Kokawa: *Scr. Mater.*, 2004, **50**, 1233–1236.
42. D. Dietrich, D. Nickel, M. Krause, T. Lampke, M. P. Coleman and V. Randle: *J. Mater. Sci.*, 2010, **46**, 357–364.